Anisotropic shell model of turbulence

Özgür D. Gürcan, Roland Grappin

Anisotropic shell model of turbulence

Ö. D. Gürcan[1,*] and R. Grappin[2,1]
[1]*Laboratoire de Physique des Plasmas, Ecole Polytechnique, CNRS, F-91128 Palaiseau Cedex, France*
[2]*Observatoire de Paris, CNRS, LUTH, F-92195 Meudon, France*
(Received 7 July 2011; revised manuscript received 3 November 2011; published 12 December 2011)

An anisotropic shell model has been proposed for two-dimensional (2D) turbulence. It is similar to the 2D version of the Gledzer-Ohkitani-Yamada model but with the angular variable in wave-number space divided into three distinct directions representing structures elongated in different directions. In the case when the drive is isotropic the usual isotropic solution is recovered as the fixed point of this model. The Hasegawa-Mima limit of the model is considered in particular due to its relevance for 2D anisotropic systems such a quasigeostrophic and plasma turbulence. It is observed from this simple model that the anisotropy diminishes as a function of scale during the cascade process, and the maximum of the energy is not at the node that has maximum drive, but at a nearby node that is directly coupled to that one.

DOI: 10.1103/PhysRevE.84.066308 PACS number(s): 47.27.E−, 52.35.Ra, 92.60.hk

I. INTRODUCTION

Shell models are commonly used as simple models for the description of the cascade processes in neutral fluids (e.g., Refs. [1–3]; see Ref. [4] for a review) and magnetohydrodynamics (MHD) [5–8]. They are based on a severe truncation of the Fourier domain, of a physical model such as the Navier-Stokes equation. Shell models usually cover a limited number of all possible interactions in the Fourier space (e.g., maybe an interaction with a large-scale flow or magnetic field component in addition to local or nearly local interactions in k space). Their naming reflects that the interactions are considered among different spherical shells of a given wave-number magnitude k in a three-dimensional (3D) k space. The idea of dividing the Fourier space into spherical shells (or equivalently integrating out the angular dependence in k space) is based on the observation that turbulence by its very nature is statistically isotropic.

However, of course, there are cases in nature where the turbulence is significantly anisotropic. This can be due to the way the turbulence is excited, or due to existence of a background large-scale flow, an externally imposed temperature difference, or a large-scale magnetic field as in the case of MHD. In fact, the fields of geophysical fluid dynamics and solar and fusion plasma physics abound with examples of anisotropic turbulence. Here we will discuss how one can address anisotropy using a sliced shell model. For simplicity, and considering the fact that both the quasigeostrophic and drift wave turbulence is better represented by this approach, we will consider a two-dimensional (2D) model. This also allows us to consider an axial anisotropy rather than a given direction of anisotropy in a 3D k space. In a sense, a 2D model already represents a 3D turbulence that is very anisotropic in the parallel versus perpendicular directions (to the extent that the parallel variations are ignored and a 2D model is used). Here we discuss the additional anisotropy in the perpendicular plane. In the case of the β plane [9], a direction is selected since the gradient of the background vorticity is in a given direction. In the case of the Hasegawa-Mima model [10], it is the gradient of background density that selects a direction in the perpendicular plane. Addressing cascade in such models thus requires a model capable of handling some amount of anisotropy also in the $k_\perp$ plane.

While we also write a 3D version of the model, we focus on the 2D one since it corresponds to a more physical type of anisotropy. The isotropic power-law solutions can be shown to solve the three-variable shell model in the case of isotropic drive. In contrast when the energy is injected anisotropically, the system isotropizes itself as the enstrophy cascades down the scale space, but not perfectly.

The rest of the paper is organized as follows. In the remainder of the Sec. I, we give a short background on shell models, in particular 2D models that are used in fluid and plasma turbulence. In Sec. II we introduce our 2D sliced shell model and discuss how the degree of anisotropy can be addressed within the framework of this model. In Sec. III we introduce a 3D version of the model. In Sec. IV we present numerical results, and conclude in Sec. V.

A. Background

Shell models are commonly described using the shell variables, which are defined by a relation of the form

$$u_n^2 = 2\int_{k_n} E(k)\,dk. \tag{1}$$

In the case of 2D Euler turbulence, we have the luxury of using the stream function (i.e., $\Phi_n = -iu_n/k_n$) as the shell variable. Starting from the Fourier transform of the 2D Euler, or Hasegawa-Mima equations, adding some possibility of linear waves, one can write

$$\frac{\partial}{\partial t}\Phi_{\mathbf{k}} + i\sigma\omega_{\mathbf{k}}\Phi_{\mathbf{k}} = \frac{1}{2}\sum_{\mathbf{p}+\mathbf{q}=-\mathbf{k}} M_{\mathbf{kpq}}\Phi_{\mathbf{q}}^*\Phi_{\mathbf{p}}^*,$$

where $M_{\mathbf{kpq}} = \frac{\hat{\mathbf{z}}\times\mathbf{p}\cdot\mathbf{q}(q^2-p^2)}{\sigma+k^2}$ are the *interaction coefficients*, with $\sigma = 0$ for the Euler equation and $\sigma = 1$ for the Hasegawa-Mima equation.

*ozgur.gurcan@lpp.polytechnique.fr

A simple shell model is obtained by dividing the k space into logarithmically spaced shells $k_n = k_0 g^n$ (where $g > 1$ defines the shell spacing), and truncating the convolution integral to include only the local interactions among neighboring shells:

$$\frac{\partial \Phi_n}{\partial t} + i\sigma\omega_n\Phi_n = \alpha\frac{k_n^4(g^2-1)}{\sigma+k_n^2}[g^{-7}\Phi^*_{n-2}\Phi^*_{n-1} - (g^2+1)g^{-3}\Phi^*_{n-1}\Phi^*_{n+1} + g^3\Phi^*_{n+1}\Phi^*_{n+2}]. \quad (2)$$

This actually reduces to the 2D version of the Gledzer-Ohkitani-Yamada [3] model for $\sigma = 0$ (with $\Phi_{n+i} = \Omega_{n+i}k_n^{-2}g^{-2i}$, where Ω is the vorticity), and to the Hasegawa-Mima shell model [11] for $\sigma = 1$. It conserves total energy

$$E = \frac{1}{2}\sum_n \left(\sigma + k_n^2\right)|\Phi_n|^2$$

and total "enstrophy"

$$W = \frac{1}{2}\sum_n k_n^2\left(\sigma + k_n^2\right)|\Phi_n|^2$$

as well as $Z = W + E$, which is called the generalized potential enstrophy for the Hasegawa-Mima case. The use of the Hasegawa-Mima (as well as Euler) system is motivated by physical problems. The anisotropy in a 2D problem can be imposed either by anisotropic external mixing or by a background inhomogeneity (as in the case of the Hasegawa-Mima system).

II. A SLICED SHELL MODEL

We start by the following observations and assumptions for the 2D Euler or Hasegawa-Mima equations:

(1) The interaction coefficient vanishes for $|q| \approx |p|$.[1]

(2) The interaction is most efficient if the two of the three interacting wave numbers (**k**, **p**, and **q**) are perpendicular (vanishes if they are parallel).

(3) It is assumed (in the spirit of a shell model) that the interactions are local.

If we choose consecutive wave numbers that are perpendicular (so that the interactions are most efficient), $k_{n-2}^2 + k_{n-1}^2 = k_n^2$, we find $g = \sqrt{(1+\sqrt{5})/2} \approx 1.272 \sim 1 + e/10$. Note that the derived model is valid for any value of g otherwise.

In the light of these observations, we define the sliced shell variables as follows:

$$\Phi_n^{(j)} \equiv \left[\frac{4}{\pi\left(\sigma + k_n^2\right)}\int_{k_n}^{k_{n+1}} dk \int_{\alpha_{j-1}}^{\alpha_j} d\alpha\, E\,(k,\alpha)\right]^{1/2},$$

where $j = \{0,1,2\} \to \{x,0,y\}$ and we choose the angles such that $\alpha_j = (2j-1)\pi/8$ [i.e., $\alpha = \arctan(k_y/k_x)$, so that $\int E(k,\alpha)dkd\alpha \equiv \frac{1}{2}v^2$]; these definitions warrant that

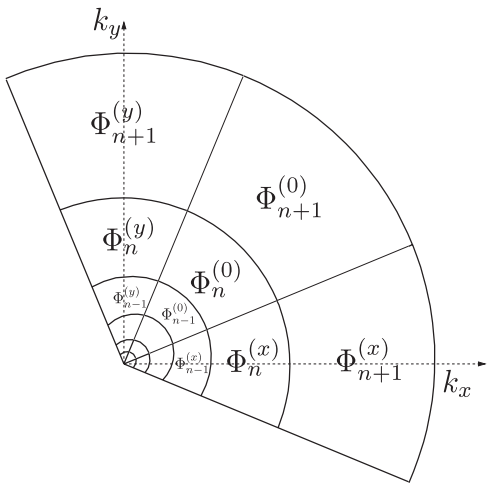

FIG. 1. The sliced shell variables of the sliced shell model in two dimensions.

$\int_{\alpha_{j-1}}^{\alpha_j} d\alpha \int_{k_{n-1}}^{k_n} dk E(k,\alpha) = (\sigma + k_n^2)|\Phi_n^{(j)}|^2$. When the unit circle is sliced this way, using mirror symmetry in k_x and k_y directions, we can describe the whole unit circle using only three variables (see Fig. 1). In other words, the unit circle is divided into two $\Phi_n^{(x)}$ and $\Phi_n^{(y)}$ type regions and four $\Phi_n^{(0)}$ type regions. The total energy and total enstrophy can be written as

$$E \equiv \sum_n \left[\left(\sigma + k_n^2\right)\left|\Phi_n^{(x)}\right|^2 + \left(\sigma + k_n^2\right)\left|\Phi_n^{(y)}\right|^2 + 2\left(\sigma + k_n^2\right)\left|\Phi_n^{(0)}\right|^2\right],$$

$$W \equiv \sum_n \left[\left(\sigma + k_n^2\right)k_n^2\left|\Phi_n^{(x)}\right|^2 + \left(\sigma + k_n^2\right)k_n^2\left|\Phi_n^{(y)}\right|^2 + 2\left(\sigma + k_n^2\right)k_n^2\left|\Phi_n^{(0)}\right|^2\right]$$

in terms of the sliced shell variables. In this formulation the variable $\Phi_n^{(x)}$ loosely represent eddies of size k_n^{-1} that are elongated in the y direction, $\Phi_n^{(y)}$ similarly but those elongated in the x direction, and $\Phi_n^{(0)}$ represent eddies that are roughly circular (e.g., see Fig. 5). Obviously these correspondences are valid only in a statistical sense and rely on the additional assumption of statistical homogeneity.

As usual in the case of the derivation of shell models, we start with a truncated system, and then use the form of the interaction coefficients and conservation laws of the original system, which are energy and enstrophy in this case. The resulting form of the anisotropic shell model can be written as

$$\frac{\partial \Phi_n^{(x)}}{\partial t} = \frac{k_n^4(g^2-1)}{\sigma + k_n^2}\left[\frac{\alpha^{(x)}}{g^7}\Phi^{(0)*}_{n-2}\Phi^{(0)*}_{n-1} - \alpha^{(0)}\frac{(g^2+1)}{g^3}\Phi^{(y)*}_{n-1}\Phi^{(0)*}_{n+1} + \alpha^{(0)}g^3\Phi^{(y)*}_{n+1}\Phi^{(0)*}_{n+2} + \beta\Phi^{(y)*}_{n}\Phi^{(0)*}_{n+1}\right], \quad (3)$$

[1] See Sec. II A on interactions with $|q| \approx |k|$.

$$\frac{\partial \Phi_n^{(y)}}{\partial t} + i\sigma\omega_n \Phi_n^{(y)} = \frac{k_n^4(g^2-1)}{\sigma + k_n^2}\left[\frac{\alpha^{(y)}}{g^7}\Phi_{n-2}^{(0)*}\Phi_{n-1}^{(0)*} - \alpha^{(0)}\frac{(g^2+1)}{g^3}\Phi_{n-1}^{(x)*}\Phi_{n+1}^{(0)*} + \alpha^{(0)}g^3\Phi_{n+1}^{(x)*}\Phi_{n+2}^{(0)*} - \beta\Phi_n^{(x)*}\Phi_{n+1}^{(0)*}\right], \quad (4)$$

$$\frac{\partial \Phi_n^{(0)}}{\partial t} = \frac{1}{2}\frac{k_n^4(g^2-1)}{\sigma + k_n^2}\left[\frac{\alpha^{(0)}}{g^7}\left(\Phi_{n-2}^{(x)*}\Phi_{n-1}^{(y)*} + \Phi_{n-1}^{(x)*}\Phi_{n-2}^{(y)*}\right) - \alpha^{(x)}\frac{(g^2+1)}{g^3}\Phi_{n-1}^{(0)*}\Phi_{n+1}^{(x)*} - \alpha^{(y)}\frac{(g^2+1)}{g^3}\Phi_{n-1}^{(0)*}\Phi_{n+1}^{(y)*} + \alpha^{(x)}g^3\Phi_{n+1}^{(0)*}\Phi_{n+2}^{(x)*} + \alpha^{(y)}g^3\Phi_{n+1}^{(0)*}\Phi_{n+2}^{(y)*}\right], \quad (5)$$

where, unlike the isotropic models, we have three different arbitrary coefficients $\alpha^{(x)}$, $\alpha^{(y)}$, and $\alpha^{(0)}$, which correspond to different classes of nonlinear interactions (in fact, $\alpha^{(0)}$ contains two different types of interactions as shown in Fig. 2).

If for the sake of argument we consider only forward cascade and focus on the terms with $\alpha^{(x)}$ in Eqs. (3)–(5), we note that they describe a large circular eddy breaking up into two eddies, a circular one and another (smaller) one elongated in the y direction. Similarly the terms proportional to $\alpha^{(y)}$ describe the large circular eddy, this time breaking up into a circular one and a smaller one elongated in the x direction. Finally the terms with $\alpha^{(0)}$ represent an eddy elongated in the x direction breaking up into smaller-scale circular eddies by the shearing of a large-scale eddy elongated in the y direction (and vice versa). If one considers inverse cascade, it is exactly the inverse processes (i.e., eddy mergers rather than breakups) that these coefficients would represent. Here β is simply the rotation of an elongated structure by a larger rotating eddy. Note, however, that, while the spatial picture is useful for having some insight into the dynamics, it is well known that this kind of basic picture is usually misleading.

Unless it is justified by the form of the interaction coefficient, one would expect $\alpha^{(x)} = \alpha^{(y)} = \alpha^{(0)}$ in the case of fully developed turbulence. This can also be justified by arguing that the interaction coefficient at a given scale is proportional to the area of the triangle involved in the interaction. One needs only to look at Fig. 2 to convince oneself that the areas of the corresponding triangles for different classes of interactions (apart from β) are indeed very close.

It is remarkable that for $\beta = 0$, a power-law solution of the form

$$\Phi_n^{(j)} = A_i k_n^{-\lambda_i} \quad (6)$$

with $\lambda_x = \lambda_y = \lambda_0 = \{4/3, 2\}$, and $A_{(x)} = A_{(0)}\alpha^{(y)}/\alpha^{(0)}$ and $A_{(y)} = A_{(0)}\alpha^{(x)}/\alpha^{(0)}$ is possible even without setting $\alpha^{(x)} = \alpha^{(y)} = \alpha^{(0)}$. These are the exact, "isotropic"[2] cascade solutions corresponding to the usual Kraichnan-Kolmogorov spectra $E(k) \propto \{k^{-5/3}, k^{-3}\}$ for the 2D Euler case (and the corresponding Hasegawa-Mima spectra in the $\sigma = 1$ case). If we consider the different classes of interactions shown in Fig. 2, that are represented by different coefficients $\alpha^{(i)}$, as "paths" in k space, through which the energy and enstrophy "flow," in this perspective, energy and enstrophy are conserved by each of these classes separately. In other words, there is no exchange of energy or enstrophy between these separate paths. This is obviously a "subset" of the general case when the energy and enstrophy are conserved as a result of such interactions and exchanges between them. In other words, in a real system if one path is full, the energy and enstrophy may switch to another path and flow up or down scale using that other path. It may be interesting to consider different weights in these different classes of interactions, with an anisotropic drive.

A. Isotropizing interactions within a shell

As discussed earlier, the interaction coefficient $M_{\mathbf{kpq}}$ vanishes exactly when $|q| \approx |p|$. This rules out interactions involving same scales. In a three-wave interaction point of view this means that if one of the waves gives energy to (or takes energy from) two other waves, the two waves that gain energy (or give energy) cannot have the same wave-number magnitude. Note, however, that the coefficient does not vanish for $q \approx k$. In other words, the wave can give energy to (or take energy from) two waves, one of which have the same wave-number magnitude as itself and another one that is larger [for instance, $\mathbf{k} = k\hat{\mathbf{x}}$ may give its energy to $\mathbf{p} = k\hat{\mathbf{y}}$ and $\mathbf{q} = \sqrt{2}k(\frac{\hat{\mathbf{x}}+\hat{\mathbf{y}}}{\sqrt{2}})$]. This interaction transfers the energy from one part of the k shell to another part, and thus it does not normally enter the standard shell model formulation. The contribution of this term, when integrated over the angular variable, would be zero. In our model this is the term that is represented by the coefficient β in (3) and (4). Obviously when we compute $I_n = |\Phi_n^{(x)}|^2 + |\Phi_n^{(y)}|^2 + 2|\Phi_n^{(0)}|^2$, which appears in any generic conservation law (i.e., $Z_n = \sigma_n I_n$, where $Z = \sum_n Z_n$ is a global conserved quantity like energy or enstrophy), and corresponds to angular averaging at a given n, the contribution from this term vanishes. This term leads to a nonlinear isotropization of a linearly anisotropic distribution of energy or enstrophy, thus sometimes used in justifying the use of isotropic spectra, even in situations where there are sources of weak anisotropy. Here we will consider $\beta = 0$ and $\beta = \pm 1$ cases separately to see the effect of this term (see Fig. 3).

Note that if we defined two separate variables that represent $\Phi_n^{(0)}$ in the first and second quadrants, a similar term would appear, transferring energy or enstrophy between the two quadrants of $\Phi_n^{(0)}$; however, since we take $\Phi_n^{(0)}$ as being already averaged over its segments in all four quadrants, the term already vanishes.

B. The anisotropy tensor

In order to study the anisotropy, one needs a measure of it. In general, in a 3D turbulent fluid, the anisotropy tensor can be used, which is defined as

$$a_{ij} = \frac{\langle \widetilde{u}_i \widetilde{u}_j \rangle}{K} - \frac{2}{3}\delta_{ij},$$

[2]Note that while the power law slopes are the same in Eq. (6), in general, due to A_i being different, the solution is not truly isotropic.

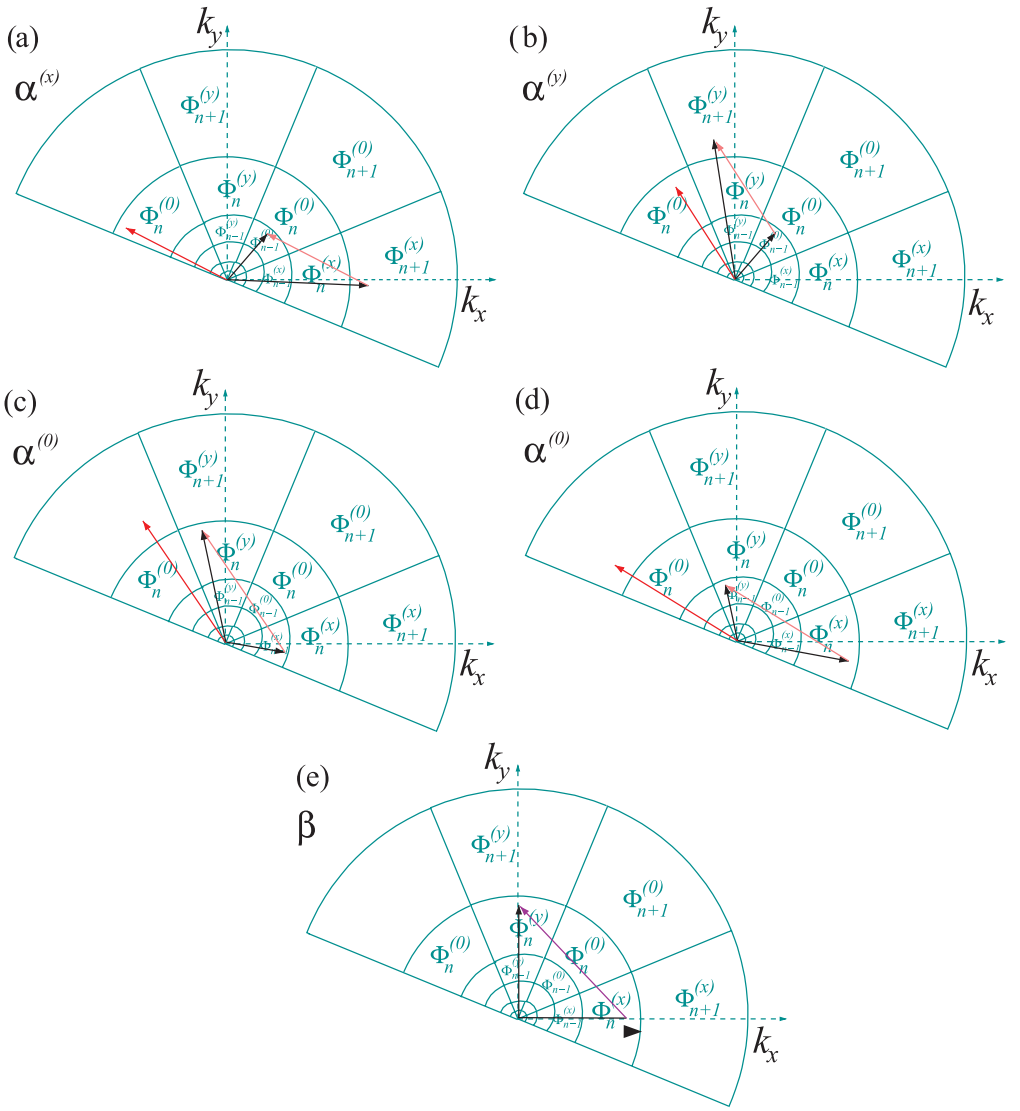

FIG. 2. (Color online) The types of triangles that are considered in Eqs. (3)–(5). Each class and their self-similar scalings are considered within the shell model and are represented by different coefficients; the triangles in (a) are represented by the interactions that appear with the coefficient $\alpha^{(x)}$, the triangles in (b) with $\alpha^{(y)}$, the triangles in (c) and (d) with $\alpha^{(0)}$, and the triangles in (e) represent the same scale interactions with coefficient β. For this last class, the third leg mediates only the energy transfer $\Phi_n^{(x)} \leftrightarrow \Phi_n^{(y)}$; it does not gain any energy. In other cases the energy and enstrophy is exchanged between all three legs of the triad.

where K is the kinetic energy. If the anisotropy has a selected direction, one usually aligns the coordinate system in parallel and perpendicular to this direction so that the anisotropy tensor becomes diagonal. For a 3D isotropic problem, $\langle \widetilde{u}_x \widetilde{u}_x \rangle = \langle \widetilde{u}_y \widetilde{u}_y \rangle = \langle \widetilde{u}_z \widetilde{u}_z \rangle$, so all the components of a_{ij} vanish. In strictly two dimensions (i.e., $\langle \widetilde{u}_z \widetilde{u}_z \rangle = 0$), one needs to define a 2D version of this tensor (this time with $\{i,j\}$ running through x and y only):

$$a_{ij} = \frac{\langle \widetilde{u}_i \widetilde{u}_j \rangle}{K} - \delta_{ij}.$$

One exceptional thing about the 2D case is that once the tensor is diagonalized (and due to imposed mirror symmetry around x and y axes the sliced shell model gives a diagonal anisotropy tensor), it remains to compute only a_{xx} (since $a_{yy} = -a_{xx}$). Note that the notation a_{xx} means $\{i,j\} = \{x,x\}$ component of the anisotropy tensor, not partial differentiation. In the shell model approach we do not have access to different components of velocity. However, one advantage of using Φ as the main variable is that we can argue for instance that $|\Phi_n^{(y)}|^2$ acts like a filter (like a 2D step function) that selects a $\mathbf{k}$ vector with $k_x \approx 0$ and $k_y \approx k$ in k space so that $k_n^2 |\Phi_n^{(y)}|^2 \sim k_y^2 \langle \widetilde{\Phi}_k^2 \rangle = \langle \widetilde{u}_{x,k}^2 \rangle$. Using this we can actually write a shell model definition of a_{xx} as

$$a_{xx,n} \equiv 2 \frac{\left|\Phi_n^{(y)}\right|^2}{\left|\Phi_n^{(x)}\right|^2 + \left|\Phi_n^{(y)}\right|^2} - 1, \tag{7}$$

which is defined as a function of scale n. You can see an example of this in Fig. 4(b), where the numerical results from a shell model is shown. Note that this is not an exact definition

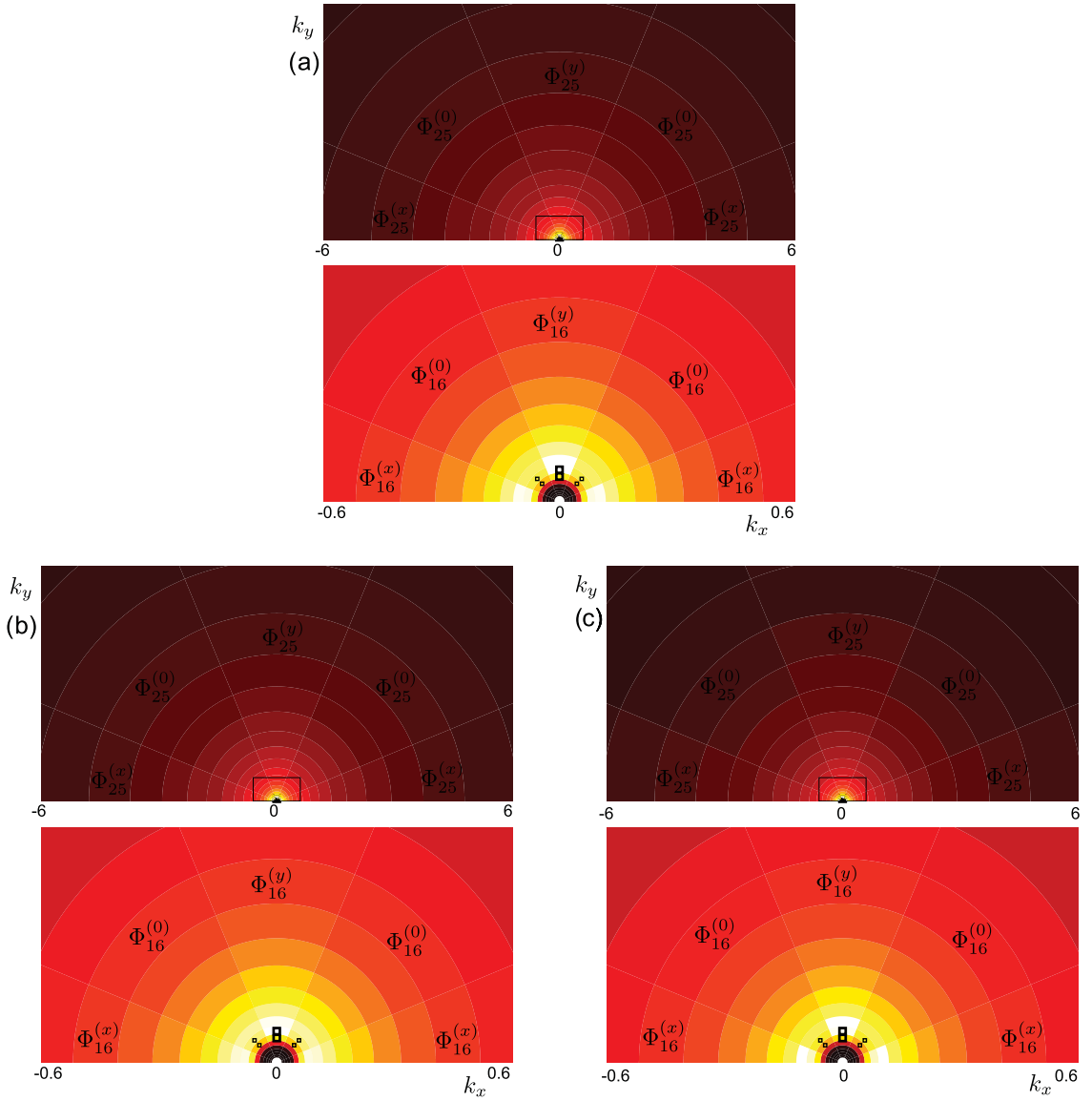

FIG. 3. (Color online) Numerical results for the 2D sliced shell model of Eqs. (3)–(5) for the case $\alpha_x = \alpha_y = \alpha_z = 1$, $g = 1.28$, $k_0 = 10^{-2}$, $\gamma = 10^{-4}$, $\nu = 10^{-7}$, and $\nu_L = 10^{-14}$. Here we can see the full spectrum as a function of k_x and k_y "reconstructed" from the sliced shell model for (a) $\beta = 0$, (b) $\beta = 1$, (c) $\beta = -1$. Some of the variables are explicitly indicated to help the reader identify the scales. The energy injection is shown by little boxes whose sizes indicate the strength of injection. As can be seen, the energy containing "scales" are slightly different from the energy injection scales. While the anisotropy clearly decreases as a function of k, some anisotropy remains even in small scales. Note that the average anisotropy as defined in Eq. (8) is 0.114 for (a) 0.137 for (b) and 0.072 for (c). The sign of $\langle a_{xx} \rangle$ indicates that there is more energy in $\Phi_{0,k}$ as compared to $\Phi_{k,0}$, which is consistent with the injection anisotropy.

of the anisotropy tensor, but an approximate shell version that can be obtained using only the shell variables.

C. Numerical results

In order to numerically implement a shell model, one has to include energy injection and dissipation, which we have not written explicitly in our model equations. This is partly due to the fact that there is usually some freedom in choosing the actual form of these terms. In the isotropic models, the energy injection is usually invoked in the first few (e.g., third and fourth) shells, where the dissipation is included in the form of $\nu k_n^m u_n$ with $m = 2$ or 4 (or even 6 or 8), and with a small enough ν in order to guarantee a large inertial range. In the sliced shell model, we inject energy at $\Phi^{(y)}_8$ and $\Phi^{(y)}_9$ at a fixed rate γ (i.e., $\frac{\partial \Phi_n}{\partial t} = \gamma + \cdots$), and in order to allow for coupling (since two consecutive y variables do not couple) we also inject some energy at a slower rate of $\gamma/10$ at $\Phi^{(0)}_8$ and $\Phi^{(0)}_9$. Since the physical model has a tendency toward inverse cascade we have to extract energy at the large scales. We do this by adding a term $-(\nu_L/k_n^8)\Phi_n^{(i)}$ in each equation with ν_L chosen such that the energy extracted at the largest scale is $O(1)$. Similarly we add a viscosity term that affects large k in the form of $-\nu k_n^4 \Phi_n^{(i)}$. We have implemented the resulting ordinary differential equations (ODEs) using an eighth-order

Runge-Kutta scheme from the Gnu Scientific Library [12], using openmp [13] and the gcc compiler to take advantage of multiprocessing capabilities. While all this is unnecessary for a shell model, any gain in speed is reflected as better statistics and thus is nonetheless desirable. The shell variables are initiated in the form of a Gaussian, with much lower energy content than the final steady state and a random initial distribution of complex phases. The model runs fast enough to permit rapid integration to long times, necessary to ensure steady state with small values of hyperviscosity coefficients. The spectra shown have been averaged over long time intervals after the steady state has been reached. Depicted in Figs. 3 and 4 is a case where we used 32 shells (i.e., a total of 96 shell variables) with the parameter values $\alpha_x = \alpha_y = \alpha_z = 1$, $\beta = 0, g = 1.28, k_0 = 10^{-2}, \gamma = 10^{-4}, \nu = 10^{-7}$, and $\nu_L = 10^{-14}$. The reconstructed spectrum is shown in Fig. 3. The power-law behavior can be seen clearly in Fig. 4(a), and the absolute value of a_{xx} is shown in Fig. 4(b) as a measure of anisotropy. Note that the anisotropy oscillates (between $u_x^2 < u_y^2$ and $u_y^2 < u_x^2$) as we go from scale to scale, so a "net" anisotropy computed across the inertial range is smaller. One interesting observation is that the anisotropy drops rapidly on both sides of the energy containing scales (around $k \approx 0.1$), especially changing sign toward larger scales.

We have also checked the dependence of the anisotropy to the variable β, by considering $\beta = 0, \beta = 1$, and $\beta = -1$ cases separately [Figs. 3(a)–3(c)]. The sensitivity of the resulting spectra and their anisotropy to this parameter seem limited, while a negative β seems to reduce the net anisotropy by about 35%, a positive β seems to increase it by about 20%. The nonlinear interactions that are responsible for the cascade do already isotropize the spectrum, so that the addition of this term does not change the dynamics substantially, but its effect is not negligible either. In any case the anisotropy seems to oscillate wildly between positive and negative values instantaneously. It is almost always the case that if one scale has one sign of anisotropy at a given time, the scale that follows has the opposite anisotropy due to the tendency of the nonlinear terms to rotate anisotropy.

The results may seem surprising in that the anisotropy as we defined it does not vanish much more rapidly as a function of scale, as the intuition from experiment and direct numerical simulations would suggest. To study this, we were led to visualize the resulting reconstructed spectra in real space. This can be done simply by taking the reconstructed spectra as depicted, for instance, in Fig. 3, adding a random phase to each point in k space and then performing the inverse fast Fourier transform. This gives a randomized (the phase information is what determines the actual spatial shape, and here this is chosen completely randomly) "realization" that is statistically consistent with the given spectrum. As one can see, the spatial distribution (even though not exactly $a_{xx} = 0$ for all scales, which would mean perfect isotropy) looks very isotropic to the eye. In contrast, if we consider the same spectrum, but setting $\Phi_n^{(x)} = \Phi_n^{(0)} = 0$ by hand (i.e., the case $a_{xx} = 1$ for all scales). We find a very anisotropic-looking spectrum. The reason for this is the fact that even though the $a_{xx,n}$ as a function of n does not vanish, since it oscillates between positive and negative values from scale to scale, on average it gives no net

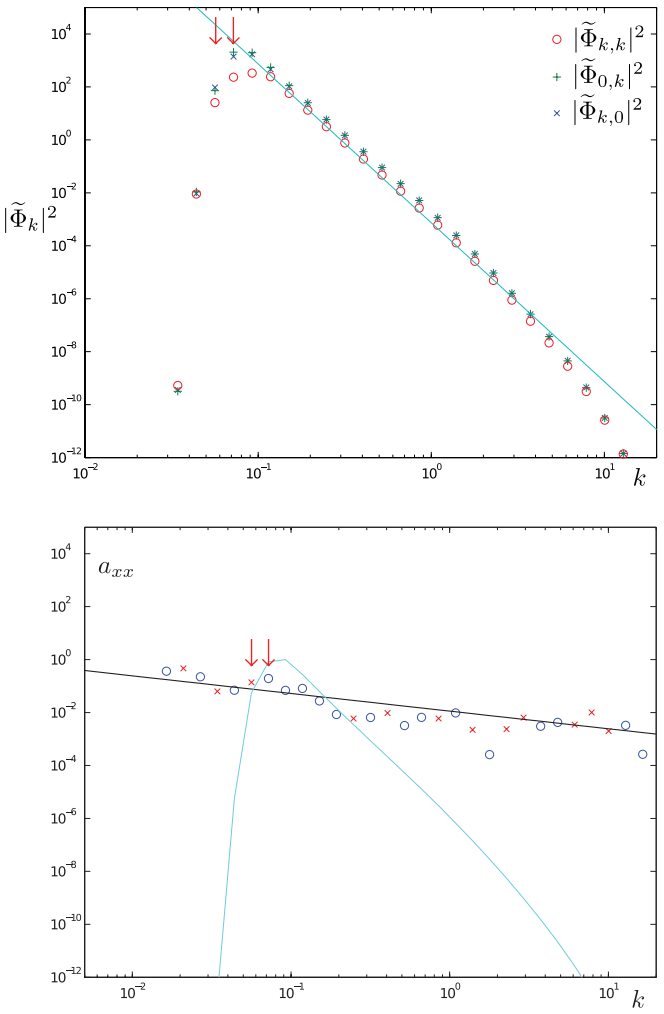

FIG. 4. (Color online) Numerical results for the 2D sliced shell model of Eqs. (3)–(5). The wave-number spectrum is seen in (a), in which k^{-6} correspond actually to $E(k) \propto k^{-5}(\sigma + k^2)$ (hence to the Kraichnan-Kolmogorov spectra for the Euler problem). However, for the Hasgawa-Mima case, spectral energy density is not a perfect power law. The displayed quantity corresponds roughly to $|\Phi_{\mathbf{k}}|^2$. The absolute value of the xx component of the anisotropy tensor is shown in (b) with circles corresponding to positive and crosses corresponding to negative values of a_{xx} (thus to positive values of a_{yy}). The $k^{-2/3}$ line is shown as a guide for the eye. Note that the net anisotropy as computed from (8) is positive since most of the energy containing scales have a positive a_{xx}.

anisotropy. In other words, the spatially observed anisotropy is not $a_{xx,n}$ but $\langle a_{xx} \rangle$, which can be defined as

$$\langle a_{xx} \rangle \equiv 2 \frac{\sum_n \left| \Phi_n^{(y)} \right|^2}{\sum_n \left(\left| \Phi_n^{(x)} \right|^2 + \left| \Phi_n^{(y)} \right|^2 \right)} - 1; \tag{8}$$

the anisotropy that we perceive in the spatial representation is apparently this quantity which corresponds to the net, or average, anisotropy across all (or in the case of clear scale separation, a large number of) scales. For the example above, the $\langle a_{xx} \rangle = 0.114$ for Fig. 5(a); in contrast, $\langle a_{xx} \rangle = 1$ for Fig. 5(b).

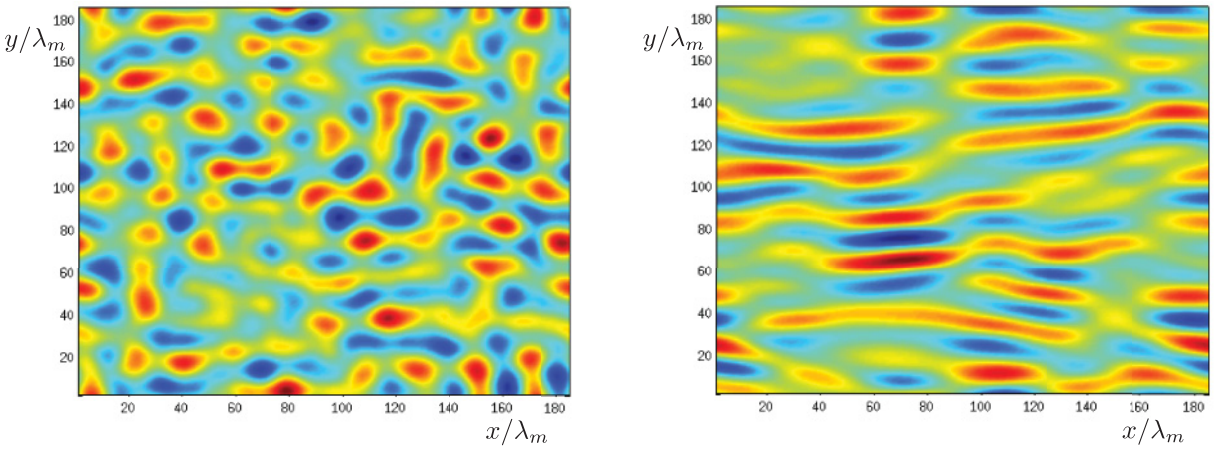

FIG. 5. (Color online) The spatial "realizations" obtained by the inverse fast Fourier transform of the reconstructed spectra (with random phase) from the shell model: (a) for the results given in Figs. 3 and 4 with $\beta = 0$ and (b) for the same case but with setting $\Phi_n^{(x)} = \Phi_n^{(0)} = 0$ by hand. Using the definition in Eq. (8), here $\langle a_{xx} \rangle = 0.114$ for (a) and by definition, $\langle a_{xx} \rangle = 1$ for (b).

III. CONCLUSION

We have developed a simple sliced shell model for axial anisotropy in homogeneous 2D turbulence, using three variables for each shell. The model can be used to describe 2D or quasi-2D turbulence when the axial symmetry is broken as in cases where there is a background inhomogeneity. We have shown that the basic form of the isotropic solution survives in the anisotropic case with anisotropic drive. Using a shell model version of the anisotropy tensor to describe the degree of anisotropy as a function of scale, we found that the absolute value of anisotropy that is extracted from the shell variables decays roughly as $k^{-2/3}$. The anisotropy is most pronounced in the energy-containing scales; however, even with an anisotropic drive, since the anisotropy oscillates from scale to scale, the net anisotropy as calculated by (8), remains feeble.

ACKNOWLEDGMENT

This work is supported by the French "Agence nationale de la recherche," contract ANR JCJC 0403 01.

[1] V. N. Desnianskii and E. A. Novikov, J. Appl. Math. Mech. **38**, 468 (1974).
[2] T. L. Bell and M. Nelkin, Phys. Fluids **20**, 345 (1977).
[3] M. Yamada and K. Ohkitani, Prog. Theor. Phys. **79**, 1265 (1988).
[4] L. Biferale, Ann. Rev. Fluid Mech. **35**, 441 (2003).
[5] C. Gloaguen, J. Leorat, A. Pouquet, and R. Grappin, Physica D **17**, 154 (1985).
[6] R. Grappin, J. Leorat, and A. Pouquet, J. Physique **47**, 1127 (1986).
[7] F. Plunian and R. Stepanov, New J. Phys. **9**, 294 (2007).
[8] T. Lessinnes, D. Carati, and M. K. Verma, Phys. Rev. E **79**, 066307 (2009).
[9] P. B. Rhines, J. Fluid Mech. **69**, 417 (1975).
[10] A. Hasegawa and K. Mima, Phys. Fluids **21**, 87 (1978).
[11] J. L. Ottinger and D. Carati, Phys. Rev. E **48**, 2955 (1993).
[12] M. Galassi *et al.*, *GNU Scientific Library Reference Manual,* 3rd ed. (Network Theory, Bristol, UK, 2009).
[13] L. Dagum and R. Menon, Comput. Sci. Eng., IEEE **5**, 46 (1998).